

Confined water layers in graphene oxide probed with spectroscopic ellipsometry

Mandakranta Ghosh, L. Pradipkanti, Vikas Rai, Dillip K. Satapathy, Pramitha Vayalamkuzhi, and Manu Jaiswal

Citation: *Applied Physics Letters* **106**, 241902 (2015); doi: 10.1063/1.4922731

View online: <http://dx.doi.org/10.1063/1.4922731>

View Table of Contents: <http://scitation.aip.org/content/aip/journal/apl/106/24?ver=pdfcov>

Published by the [AIP Publishing](#)

Articles you may be interested in

[Influence of transfer residue on the optical properties of chemical vapor deposited graphene investigated through spectroscopic ellipsometry](#)

J. Appl. Phys. **114**, 093505 (2013); 10.1063/1.4819967

[Large-area microfocal spectroscopic ellipsometry mapping of thickness and electronic properties of epitaxial graphene on Si- and C-face of 3C-SiC\(111\)](#)

Appl. Phys. Lett. **102**, 213116 (2013); 10.1063/1.4808379

[Spectroscopic imaging ellipsometry and Fano resonance modeling of graphene](#)

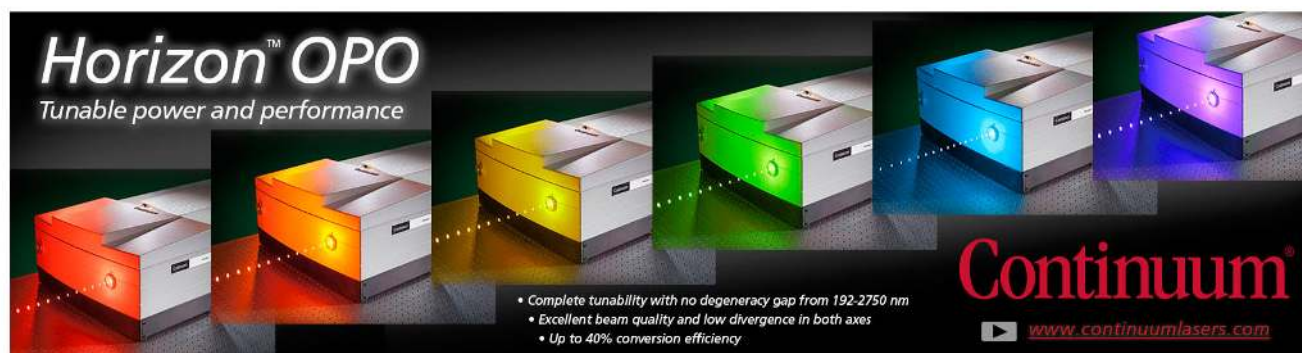
J. Appl. Phys. **112**, 123523 (2012); 10.1063/1.4771875

[Optical and structural characterization of epitaxial graphene on vicinal 6H-SiC\(0001\)-Si by spectroscopic ellipsometry, Auger spectroscopy, and STM](#)

J. Vac. Sci. Technol. B **30**, 04E106 (2012); 10.1116/1.4726199

[Kinetic investigation of copper film oxidation by spectroscopic ellipsometry and reflectometry](#)

J. Vac. Sci. Technol. A **18**, 2527 (2000); 10.1116/1.1287156



Horizon™ OPO
Tunable power and performance

• Complete tunability with no degeneracy gap from 192-2750 nm
• Excellent beam quality and low divergence in both axes
• Up to 40% conversion efficiency

Continuum®
www.continuumlasers.com

Confined water layers in graphene oxide probed with spectroscopic ellipsometry

Mandakranta Ghosh,¹ L. Pradipkanti,¹ Vikas Rai,¹ Dillip K. Satapathy,¹ Pramitha Vayalamkuzhi,² and Manu Jaiswal^{1,a)}

¹Department of Physics, Indian Institute of Technology Madras, Chennai 600036, India

²Department of Electrical Engineering, Indian Institute of Technology Madras, Chennai 600036, India

(Received 24 April 2015; accepted 7 June 2015; published online 16 June 2015)

The confinement of water in quasi two-dimensional layers is intriguing because its physical properties can be significantly different when compared to those of the bulk fluid. This work describes spectroscopic ellipsometry study of confined water layers trapped between sheets of graphene oxide at varied thermal annealing temperatures. The wavelength-dependent refractive index of graphene oxide changes abruptly with annealing temperatures for $T_{\text{ann}} \approx 125\text{--}160\text{ }^\circ\text{C}$, and we demonstrate that these changes are primarily governed by the expulsion of trapped water. This expulsion is associated with the decrease of interlayer separation of graphene oxide sheets from 7.8 \AA to 3.4 \AA . Graphene oxide annealed at high temperatures lacks trapped water layers and robust estimates of refractive index can be obtained within a Lorentz oscillator model. The trends in oscillator parameters are extended to lower annealing temperatures, where trapped water is present, in order to estimate the refractive index of confined water, whose value is found to be enhanced as compared to that of bulk. Temperature-dependent ellipsometry data show anomalous changes in ellipsometric parameters over a wide temperature interval (-10 to $10\text{ }^\circ\text{C}$) about the ice-point and these may be attributed to possible phase transition(s) of confined water. © 2015 AIP Publishing LLC. [<http://dx.doi.org/10.1063/1.4922731>]

Water in its bulk three-dimensional form is an interesting system with a complex phase diagram. The confinement of water further lends a new dimension to the range of configurations that this system can take.^{1–3} The structure and dynamics of interfacial water are remarkably different from that of bulk.¹ This has relevance for diverse systems such as water near a cell membrane or for interfacial fluids in industrial processes like lubrication and filtration.^{1,4} In two-dimensions (2D), the confinement of water becomes particularly interesting with reference to the liquid-solid phase transition because Mermin-Wagner theorem precludes the formation of long-range crystalline order.⁵ The melting phase transition in confined water has been predicted in terms of a sequence of two continuous transitions.⁶ Graphene oxide (GO) is a particularly interesting confining wall for water molecules because the spatial density of oxygen-rich surface groups can be tuned using thermal annealing or exposure to chemical vapors.^{7,8} It is well known that layered GO films prepared from aqueous solutions contain trapped water.^{7,9} A single GO sheet comprises of a mosaic of hydrophilic and hydrophobic regions, where the former strongly interact with trapped water and serve as crucial spacers for the latter.⁹ The network of water-containing quasi-2D hydrophobic nanocapillaries allows superpermeation of water molecules remarkably even as the GO membrane blocks the flow of helium gas.⁹ A recent transmission electron microscopy study of quasi-2D water layer deliberately trapped between hydrophobic atomically thin pristine graphene membranes has revealed the presence of square-ice.¹⁰

In this work, we use spectroscopic ellipsometry (SE) to study GO films, whose degree of reduction as well as water content is controllably varied by means of thermal annealing. The optical properties of GO have attracted interest because of its applications in optoelectronics and solar energies.¹¹ Previous investigations of GO using ellipsometry have not explicitly considered the role of trapped water while investigating the optical properties of this system.^{8,12} One previous study based on ellipsometry techniques has considered an optical model comprising successive layers of graphene oxide sheets and trapped water.⁷ However, even in that work, the properties of trapped water were assumed to be the same as those of bulk water.⁷ Here, we demonstrate that it is the expulsion of water rather than change in chemical structure of GO that determines the most important changes in refractive index of GO films as function of annealing temperature. GO films annealed at higher temperatures lack the complexity introduced by the presence of confined water. An estimate of the refractive index of confined water layer, when present, is obtained within an effective-medium approximation (EMA) model by extending the trends in variation of Lorentz oscillator parameters obtained for water-free GO systems. Temperature-dependent ellipsometry is used to probe the response of this system in the vicinity of ice-point of bulk water.

Graphene-oxide (GO) thin-films are prepared by spin-coating 1 mg/ml aqueous suspension on piranha-cleaned SiO_2/Si substrate. Thermally annealed samples are prepared by heating GO samples under Ar flow ($70\text{ sccm}/30\text{ min}$). Scanning electron microscopy reveals GO flake sizes between 0.5 and $5\text{ }\mu\text{m}$. Fig. 1 shows X-ray diffraction data of GO films as a function of annealing temperature varied

^{a)}Email: manu.jaiswal@iitm.ac.in

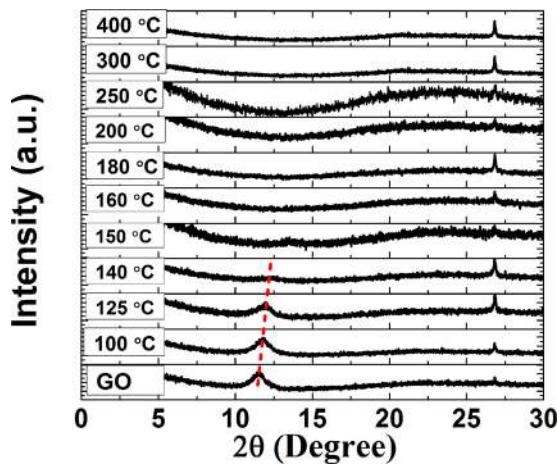


FIG. 1. XRD data of as-prepared GO and thermally reduced GO at different annealing temperatures.

between $T_{\text{ann}} = 30^\circ\text{C}$ (as-prepared) to $T_{\text{ann}} = 400^\circ\text{C}$. The as-prepared sample shows a prominent peak at 11.5° , which corresponds to c -axis separation of 7.8 \AA , while a much smaller peak at 27° indicates that some low fraction of the material exists in graphitic state too, with c -axis separation of 3.4 \AA . The existence of interlayer separations $d > 3.4 \text{ \AA}$ can be attributed to the presence of oxygen-containing functional groups.⁹ After GO film is subject to annealing at varying temperatures, the dominant peak at 11.5° gradually undergoes a slight shift to higher angles, which can be associated with decrease in interlayer separation from 7.8 \AA (as-prepared) to 6.6 \AA (for $T_{\text{ann}} = 150^\circ\text{C}$). For $T_{\text{ann}} = 160^\circ\text{C}$, graphitic peak at 27° is intense, while the peak at 11.5° is clearly absent. The controlled annealing of GO provides a suitable knob to tune interlayer separation of GO sheets by means of elimination of functional groups. MD simulations have indicated that a monolayer of water requires $d > 6 \text{ \AA}$ separation between the confining graphene sheets, and the water monolayer cannot exist for smaller partitions. This rules out presence of trapped water for higher annealing temperatures ($T_{\text{ann}} \geq 180^\circ\text{C}$).⁹ In the SE studies discussed below, we consider two categories of GO samples based on their interlayer separations and the resultant ability to accommodate trapped water layer.

The SE measurements are performed using M-2000VI rotating compensator ellipsometer (J.A. Woollam Co.) with spectral range of $370\text{--}1800\text{ nm}$ and 75° incident angle. Temperature-dependent SE data are obtained between 25°C and -10°C using M-2000 V in the spectral range of $370\text{--}1000\text{ nm}$ and 70° incident angle. The sample is kept under N_2 -gas atmosphere and data are measured after stabilizing the temperature with an accuracy of 0.1°C . Ellipsometry involves measurement of change in polarization from plane-polarization to elliptical polarization for light obliquely incident on a thin-film. The ellipsometric parameters $\{\psi, \Delta\}$ can be related to complex reflection coefficients of light parallel and perpendicular to the plane of incidence R_p and R_s , respectively: $R_p/R_s = \tan \psi \exp(i\Delta)$. Here, $\tan \psi$ represents the amplitude ratio and Δ represents the phase difference.¹³ Wavelength-dependent optical constants (n, k) and thickness of the film can be extracted from $\{\psi, \Delta\}$ by developing an optical dispersion model of the material.¹³ To analyze the SE

data, a 4-layer optical model is built that comprises the GO film and the SiO_2/Si substrate, while an interface layer between the thermal SiO_2 and Si is also included.¹⁴ The optical constants and thickness of GO film are investigated subsequent to SE characterization of bare SiO_2/Si substrate. To quantify how well the model-generated data matches with experimental data, root mean squared error (MSE) is used. For $T_{\text{ann}} \geq 180^\circ\text{C}$, GO films are considered as homogeneously composed of layered GO sheets lacking trapped-water. A Lorentz oscillator model with Kramers-Kronig (KK) transformation is used for that layer since GO has significant absorption in visible wavelength region.^{8,12} The general expression for the Lorentz oscillator model comprising of k -oscillators is given by

$$\epsilon(\lambda) = \epsilon_\infty + \sum_k \frac{A_k}{E_k^2 - \left(\frac{hc}{\lambda}\right)^2 - iB_k\left(\frac{hc}{\lambda}\right)}, \quad (1)$$

where $\epsilon(\lambda)$ is the wavelength-dependent dielectric constant and ϵ_∞ is a constant offset for approximating the effect of absorptions which are significantly distant from the measured wavelengths. A_k , E_k , and B_k represent amplitude, center energy, and energy spread of the k th oscillator, respectively.⁸ The optical constants (n, k) are related to the dielectric constant $\epsilon(\lambda)$ and they are directly extracted. As discussed above, for $T_{\text{ann}} < 180^\circ\text{C}$, a composite system of GO and trapped water is present, and therefore, any physical oscillator parameterization is not feasible. This GO layer is modeled well with B-Spline function with KK-transformation consistency.¹⁵

A plot of $n(\lambda)$ for GO samples annealed at different temperatures is shown in Fig. 2. The solid curves represent Lorentz oscillator parameterized curves, while the dashed curves represent data modeled with B-Spline. The $n(\lambda)$ curves for GO annealed at $T_{\text{ann}} \geq 180^\circ\text{C}$ progressively shift towards the standard graphite curve (CompleteEASE library). Significant changes in $n(\lambda)$ occur in the temperature interval between 125 and 160°C . The $n(\lambda)$ changes from being nearly wavelength-independent at lower annealing temperatures ($T_{\text{ann}} \leq 125^\circ\text{C}$) to become graphite-like at higher annealing temperatures ($T_{\text{ann}} \geq 180^\circ\text{C}$). These abrupt changes in $n(\lambda)$

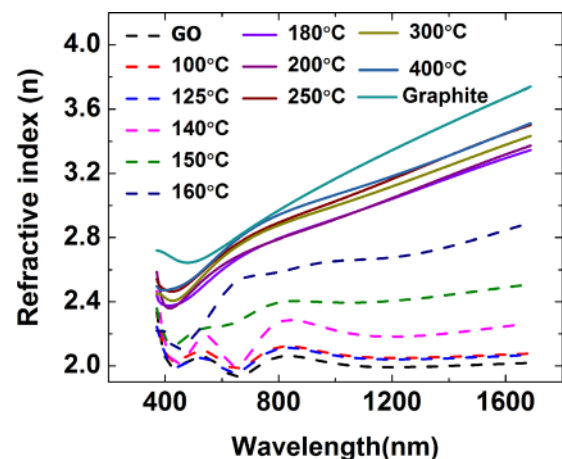


FIG. 2. Refractive index vs. wavelength for as-prepared GO and GO annealed at different temperatures.

over a narrow annealing temperature interval can have two contributing factors: (a) the chemical structure of GO undergoes abrupt changes in the above temperature interval and (b) it is the expulsion of trapped water that primarily determines these changes. To explore the first possibility, Micro-Raman spectroscopy measurements on GO films were performed using Horiba HR-800-UV ($\lambda_{\text{laser}} = 632.8 \text{ nm}$). The ratio of integrated area of defect-peak at $\sim 1338 \text{ cm}^{-1}$ with the G-peak at $\sim 1585 \text{ cm}^{-1}$, I_D/I_G is plotted in Fig. 3(a). Importantly, these measurements reveal that defects, mainly oxygen-rich groups, are gradually eliminated by annealing across the entire temperature regime (100–400 °C).¹⁶ This brings us to the second possibility that it is trapped water expulsion that determines these large changes in $n(\lambda)$. A previous SE study has used bulk optical constants of water ($n = 1.33$), to extract the “intrinsic” GO refractive index within a multilayered model.⁷ First, this assumption of bulk properties for water is not justified in light of the recent discovery of dense square-ice at room temperature (lattice constant, 2.8 Å) for water deliberately trapped between pristine graphene layers.¹⁰ Furthermore, if the intervening layer between GO sheets is presumed to be bulk-water, then the extracted “intrinsic” refractive index of GO shows significant abrupt changes in the temperature regime between $T_{\text{ann}} = 125\text{--}160 \text{ °C}$. An assumption of bulk-water optical constants for the GO: water layered

system, therefore, leads to an unsatisfactory conclusion that discontinuous changes in extracted “intrinsic” GO refractive index occur upon increase of annealing temperature even as chemical structure of GO shows gradual changes. We therefore suggest that it is the expulsion of trapped water layers that primarily governs the abrupt changes in refractive index of the system, with a small contribution arising from the change in chemical structure of GO. The quantitative estimates of respective contributions are discussed below.

We next consider the evaluation of optical constants of confined water trapped between the GO sheets. For this, the layer of GO is modeled as a known system with the properties of water layer being treated as unknown. As discussed above, the n, k values of GO for $T_{\text{ann}} \geq 180 \text{ °C}$ can be readily modeled with three Lorentz oscillators [yielding solid $n(\lambda)$ curves shown in Fig. 2]. This represents the situation where trapped water has been expelled. The gradual changes in $n(\lambda)$ for $T_{\text{ann}} \geq 180 \text{ °C}$ can be accounted as arising due to chemical structure changes of GO. By extending the trends in variation of oscillator parameters to lower T_{ann} , quantitative estimates of the contributions to the total changes in $n(\lambda)$ of the film arising from chemical structure changes of GO sheets can be discerned. For the samples at lower annealing temperatures (for $T_{\text{ann}} < 180 \text{ °C}$), we approximate oscillator parameters of each individual Lorentz oscillator at that temperature by linear extrapolation of the trend in variation of center energy, amplitude, and energy spread measured at higher annealing temperatures, as shown in Fig. 3(b), for the case of oscillator energies. The three oscillator energies (for, e.g., $C_1 \sim 2.3 \text{ eV}$, $C_2 \sim 3.6 \text{ eV}$, and $C_3 \sim 0.7 \text{ eV}$ for 400 °C annealed sample) can be correlated with energy separations in the local density of electronic states of GO associated with the presence of hydroxyl and other oxygen-containing groups.¹⁷ The linear fits shown in Fig. 3(b) can then be interpreted as accounting for changes in the chemical structure of GO due to elimination of oxygen-containing defects upon annealing. For GO: water layered system, thickness estimates are first obtained using B-Spline fits to raw SE data. We then model the system using Bruggeman EMA, which is applicable for two-phase composite systems.¹⁸ Here, the intrinsic GO represents a medium, whose oscillator energy parameters are obtained by the linear fits described above, while the confined water is considered as a Cauchy medium ($k = 0$), whose refractive index and volume fraction are determined as fitting parameters. Within this EMA model, a plot of $n(\lambda)$ for confined water is shown in Fig. 3(c). The significant increase ($\sim 35\%$) of $n(\lambda)$ of trapped water from bulk values can be attributed to confinement induced densification of the liquid related to water-wall interaction and altered water-water interaction.⁵ Similar trends in $n(\lambda)$ of confined water are obtained for GO films subject to different annealing temperatures. Note that each curve in Fig. 3(c) has been generated using input from samples prepared under identical conditions but annealed at different temperatures. The estimated error due to fitting procedure, $\Delta n \sim 0.1$, which is comparable to the spread in $n(\lambda)$ curves and can be attributed to sample-to-sample variations, for, e.g., in layer numbers/amount of trapped water. The intrinsic n_{GO} , k_{GO} of GO sheets for $\lambda = 600 \text{ nm}$ are plotted as a function of T_{ann} in

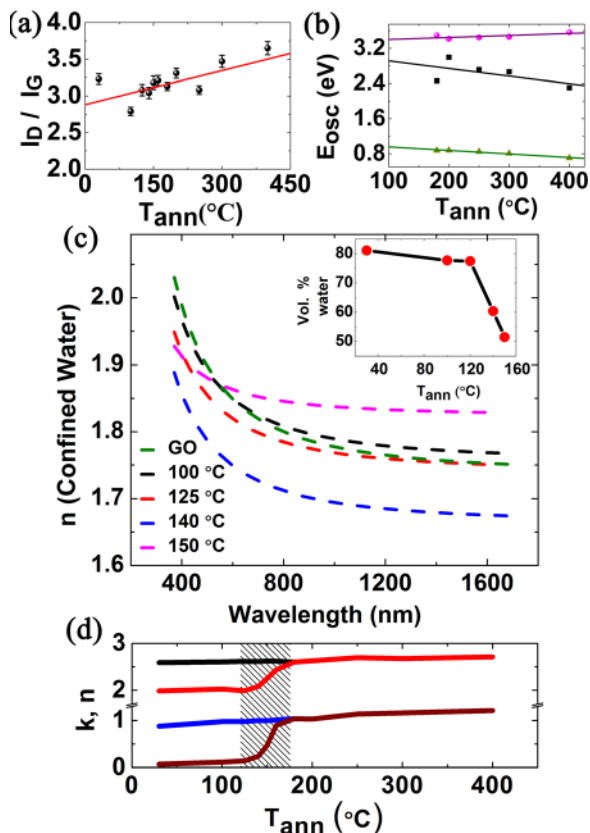


FIG. 3. (a) I_D/I_G vs. T_{ann} . Red line is a guide to the eye. (b) Variation of oscillator energies [C_1 (black squares), C_2 (red circles), and C_3 (green triangles)] for thermally annealed GO at different T_{ann} . Solid lines are linear extrapolation of energy values to lower annealing temperatures (c) $n(\lambda)$ for confined water for GO films annealed at various temperatures. [Inset: volume percentage of confined water vs. T_{ann}] (d) Intrinsic n_{GO} (black), k_{GO} (blue), and total n (red), k (brown) vs. T_{ann} for $\lambda = 600 \text{ nm}$. Dashed region denotes temperature interval where water is expelled.

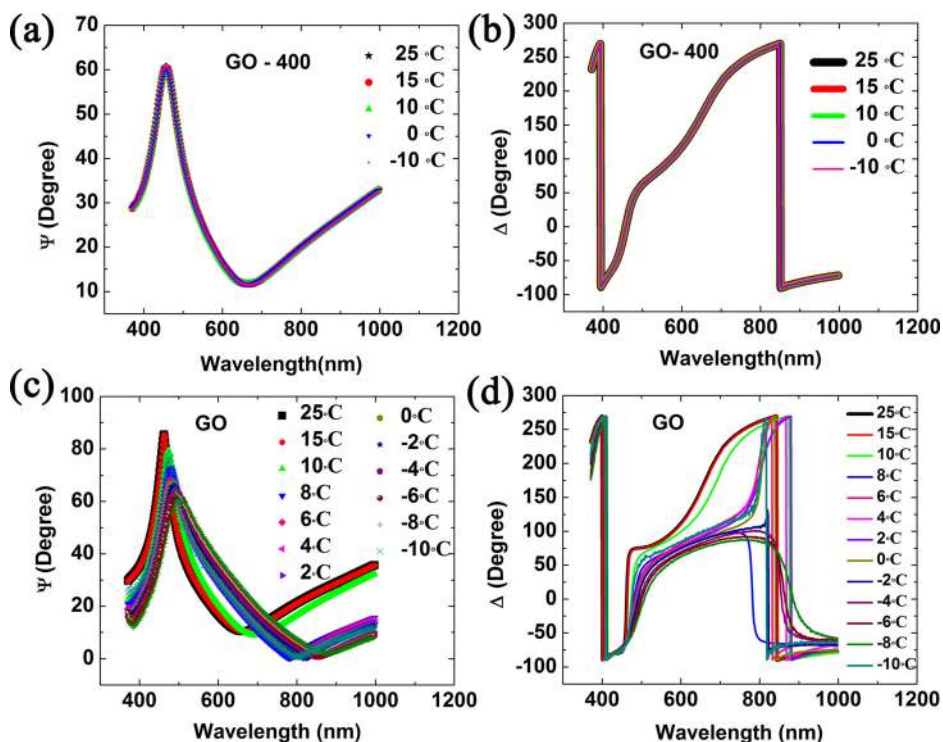


FIG. 4. Temperature-dependent ψ and Δ for 400 °C annealed GO and as prepared GO are shown in (a)–(d), respectively.

Fig. 3(d) and show gradual changes which can be related to the elimination of oxygen-containing groups and change of chemical structure of GO. In contrast, the total $\{n, k\}$ of the film, which also include the water contribution, have abrupt increases in a narrow T_{ann} interval [Figs. 2 and 3(d)]. This is rationalized only as a consequence of change in the volume percentage of water in the GO films, as plotted in the inset of Fig. 3(c). The progressive expulsion of confined water layers for $T_{\text{ann}} = 125\text{--}150\text{ }^{\circ}\text{C}$ can be clearly seen.

Finally, we discuss *temperature-dependent* ellipsometry data for GO films, measured in the temperature range from 25 °C to $-10\text{ }^{\circ}\text{C}$. Plots of ellipsometric parameters $\{\psi, \Delta\}$ for water expelled GO film annealed at 400 °C shown in Figs. 4(a) and 4(b) reveal nearly temperature-independent data. The ellipsometric parameters $\{\psi, \Delta\}$ for as-prepared GO are plotted in Figs. 4(c) and 4(d). These data reveal significant changes in the temperature interval 10 °C to $-10\text{ }^{\circ}\text{C}$. Such large changes at low temperatures cannot be related to chemical structure changes of GO sheets because (a) these changes are absent in high-temperature (400 °C) annealed GO and (b) there is no physical basis for such an explanation. The most plausible explanation for these changes is therefore in relation to the confined water. It may be noted that MD simulations have predicted marked variations of the liquid-solid phase transitions in confined water films with densification of the fluid being the determining factor for onset of the phase transition.⁵ In view of these theoretical predictions, we attribute the observed changes to possible phase transition(s) of confined water layers. This temperature-dependent ellipsometry data corroborate the important role of confined water in GO system, already inferred from our annealing studies. A detailed interpretation of the possible phase(s) of confined water system trapped in GO is beyond the scope of this work.

In conclusion, spectroscopic ellipsometry study of GO films reveals intriguing aspects about confined water layers interspersed between the GO sheets. The interlayer separations of GO sheets are controlled with thermal annealing, and trapped water layers can also be completely expelled at high annealing temperatures. The water expulsion primarily determines the refractive index changes of GO films as annealing temperatures are increased. An estimate of the refractive index for confined water is obtained and it is found to deviate considerably from the values of bulk water. This is further corroborated by extensive changes in ellipsometric parameters at temperatures deviating from the liquid-solid freezing transition of bulk water, observed in GO samples having confined water layers. Our work provides a platform to explore the exotic nature of different phases of confined-water systems.

M.J. thanks financial support from IIT-M NFSC, Nissan NRSP, and DST. P.V. thanks DST for financial support. D.K.S. thanks financial support from Nissan NRSP. The use of facilities at CNRP funded by DeitY is acknowledged. We thank R. Lakshmi and Aruna Nair for assistance.

¹S. Granick, *Science* **253**(5026), 1374 (1991).

²V. Bianco and G. Franzese, *Sci. Rep.* **4**, 4440 (2014).

³S. Chodankar, E. Perret, K. Nygård, O. Bunk, D. K. Satapathy, R. M. Espinosa-Marzal, T. E. Balmer, M. Heuberger, and J. F. van der Veen, *EPL* **99**(2), 26001 (2012).

⁴P. Kélicheff and O. Spalla, *Langmuir* **10**(5), 1584 (1994).

⁵S. Han, M. Y. Choi, P. Kumar, and H. E. Stanley, *Nat. Phys.* **6**, 685 (2010).

⁶K. J. Strandburg, *Rev. Mod. Phys.* **60**, 161 (1988).

⁷I. Jung, M. Vaupel, M. Pelton, R. Piner, D. A. Dikin, S. Stankovich, J. An, and R. S. Ruoff, *J. Phys. Chem. C* **112**(23), 8499 (2008).

⁸Y. Shen, P. Zhou, Q. Q. Sun, L. Wan, J. Li, L. Y. Chen, D. W. Zhang, and X. B. Wang, *Appl. Phys. Lett.* **99**, 141911 (2011).

⁹R. R. Nair, H. A. Wu, P. N. Jayaram, I. V. Grigorieva, and A. K. Geim, *Science* **335**, 442 (2012).

- ¹⁰G. Algara-Siller, O. Lehtinen, F. C. Wang, R. R. Nair, U. Kaiser, H. A. Wu, A. K. Geim, and I. V. Grigorieva, *Nature* **519**, 443 (2015).
- ¹¹K. K. Manga, S. Wang, M. Jaiswal, Q. Bao, and K. P. Loh, *Adv. Mater.* **22**, 5265 (2010).
- ¹²K. G. Zhou, M. J. Chang, H. X. Wang, Y. L. Xie, and H. L. Zhang, *J. Nanosci. Nanotechnol.* **12**, 508 (2012).
- ¹³H. Fujiwara, *Spectroscopic Ellipsometry: Principles and Applications* (John Wiley and Sons Ltd., Chichester, 2007).
- ¹⁴C. M. Herzinger, B. Johs, W. A. McGahan, J. A. Woollam, and W. Paulson, *J. Appl. Phys.* **83**(6), 3323 (1998).
- ¹⁵J. W. Weber, V. E. Calado, and M. C. M. van de Sanden, *Appl. Phys. Lett.* **97**, 091904 (2010).
- ¹⁶F. Tuinstra and J. L. Koenig, *J. Chem. Phys.* **53**, 1126 (1970).
- ¹⁷D. W. Boukhvalov and M. I. Katsnelson, *J. Am. Chem. Soc.* **130**(32), 10697 (2008).
- ¹⁸F. J. Nelson, V. K. Kamineni, T. Zhang, E. S. Comfort, J. U. Lee, and A. C. Diebold, *Appl. Phys. Lett.* **97**, 253110 (2010).